ORIGINAL RESEARCH ARTICLE

Effect of Nitrogen Pressure and Substrate Bias Voltage on Structure and Mechanical Properties of Vacuum Arc Deposited VN Coatings

A.S. KUPRIN, A. GILEWICZ, G.N. TOLMACHOVA, I.O. KLIMENKO, I.V. KOLODIY, R.L. VASILENKO, and B. WARCHOLINSKI

The binary vanadium–nitrogen (V–N) coatings were formed using cathodic arc evaporation. Two sets of coatings were produced using: (a) nitrogen pressure (p_{N2}) from 0.001 Pa to 3 Pa at a constant substrate bias voltage (U_B) of − 100 V and (b) a substrate bias voltage from − 50 to − 300 V at a constant nitrogen pressure of 1.5 Pa. The influence of the above parameters on the coating properties, in particular on the insufficiently investigated and described adhesion of the coatings to the substrate, was demonstrated. The phase transformation V → V + V2N → V + c-VN → h-VN → h-VN + c-VN and c-VN → h-VN occurs for coatings formed with increasing nitrogen pressure and substrate bias voltage, respectively. With the increase in p_{N2} and U_B, an increase in coating hardness and adhesion to the substrate is observed, as well as an improvement in wear resistance.

https://doi.org/10.1007/s11661-023-07177-8

I. INTRODUCTION

TRANSITION metal compounds with nitrogen, carbon or a mixture of carbon and nitrogen form the coatings with high hardness and wear resistance. Due to such properties, the above-mentioned coatings are used in many fields, mainly as a protective coatings on tools and machine parts.[1,2] The chromium and titanium based coatings were among the first to be used as protective coatings and are still used today. Due to the large number of publications devoted to them, it may be assumed that they are probably the best studied among transition metal nitrides. Similar protective properties are also exhibited by other transition metal nitrides: MoN, NbN, ZrN, VN.

One of the most interesting and relatively rarely studied coating is the vanadium-nitrogen (V–N) system. The melting point of chromium (Cr) is 1870 °C. The melting point of vanadium is similar and is about to − 1910 °C. The phase diagrams Cr-N[3] and V–N[4] are also similar. They show that, as in the case of CrN, there are two stable phases in the V–N system: hexagonal V_2N and cubic VN. They show high hardness as well as wear resistance.

Thin nitride coatings of transition metal compounds are formed mainly by the physical vapor deposition (PVD) method. The VN coatings are formed by both methods. PVD methods include: magnetron sputtering,[5–16] cathodic arc evaporation,[17,18] pulsed laser deposition,[19,20] reactive electron beam evaporation,[21] high power impulse magnetron sputtering (HiPIMS).[22] Cathodic arc evaporation (CAE) is characterized by a high degree of plasma ionization and a high kinetic energy of ions compared to other methods of coating synthesis.[23] Therefore, the formation of the coatings by CAE technique due to the unquestionable advantages of high density and good adhesion to metal substrates is widely used. Chemical Vapor Deposition (CVD) deposition method is also applied for VN coatings.[24,25]

It is known that the technological parameters of coating formation, *e.g.,* substrate bias voltage, reactive gas pressure, arc current, substrate temperature, rotational speed of substrate holder, source-substrate distance strongly affect the properties of coatings.[6,11,23,26] The coating deposition rate, their structure and preferred orientation, chemical composition, mechanical and especially tribological properties are influenced, among others, by the substrate bias voltage and gas pressure. Thus, these are the parameters that enable the desired coating properties to be obtained. Another factor in the formation of coatings is technology applied. In the case of formation of transition metal

A.S. KUPRIN, G.N. TOLMACHOVA, I.O. KLIMENKO, I.V. KOLODIY, and R.L. VASILENKO are with the National Science Center Kharkiv Institute of Physics and Technology, Kharkiv 61108 Ukraine. A. GILEWICZ and B. WARCHOLINSKI are with the Koszalin University of Technology, Faculty of Mechanical Engineering, 75-453 Koszalin, Poland. Contact e-mail: bogdan.warcholinski@tu.koszalin.pl
Manuscript submitted March 24, 2023; accepted August 16, 2023.
Article published online August 30, 2023

nitride films using magnetron sputtering, the working atmosphere is mixture of nitrogen N_2 and argon Ar gases.[10,12–16] Few studies present the results of tests of coatings formed in the atmosphere of pure nitrogen, and rather as single samples.[17,18,27] There are also published papers presenting the results of tests of VN coatings with addition of other elements[1,16,28–30] and multilayer coatings.[2,31–34]

The VN coatings are tested relatively rarely compared to other transition metal nitride coatings. At elevated temperature oxidation of the coating may occur.[35] This is due to *e.g.,* friction between the tool and the workpiece. The formed V_2O_{2n-1} or V_2O_{2n+1} vanadium oxides with n from 3 to 6 are characterized by easy crystallographic shear planes with reduced binding strength.[20] This leads to a noticeable improvement in the tribological properties of coatings, especially at elevated temperature.

Structure[5–7,9–17,19,35,36] and basic mechanical properties, such as hardness[5–7,10–13,15–17,27,36–38] and Young's modulus[10–12,16,17,27,37] were the most frequently studied properties of the V–N coatings. Friction[11,12,17,18,27] and wear of the above coatings[11,12,17,18,21,27,39] were less frequently studied. The friction tests were performed on V–N coatings synthesized by magnetron sputtering[11,12,37] and multi-arc ion plating[17,18] by ball-on-disc[11,12,17] and reciprocating ball-on-plate[18,37] tests. The Al_2O_3[17,18,37] and 100Cr6 steel balls[11,12] were used as counterparts. In the tests, relatively small normal loads were applied (*i.e.,* 2 N,[11,12,37] 5 N[17,37] and 10 N[18]) as well as sliding speeds of 0.02 m/s[17] and 0.05 m /s.[11,12,37] The coefficient of friction and the wear rate were evaluated in a test on a sliding distance of 200 m[11,12,17,18] and 1000 m.[37]

There are few reports on the adhesion of coatings[17,27] and they concern only two compositions corresponding to the phases V_2N and VN. The test results for V–N coating systems synthesized at different nitrogen pressures are presented in a few reports.[5,6,11,13,27] There is no systematic research on the mechanical properties of coatings formed in a breath of nitrogen pressures, especially by cathodic arc evaporation.

The $Cr_{1-x}V_xN$ coatings we previously studied were characterized by a decrease in both the coefficient of friction and wear with increasing V content in the coating.[40] In the absence of systematic studies of V–N coatings synthesized in a wide range of nitrogen pressures and substrate bias voltage, especially with regard to one of their most important properties (adhesion) determining industrial applications, we undertook the subject area of optimizing coating formation and finding a relationship between the properties of coatings synthesized by cathodic arc evaporation, and technological parameters. An effect of above parameters on the coatings morphology, structure, mechanical and tribological properties was shown. Particular attention has been paid to the so far poorly described adhesion of the coatings to the substrate. The correlation of the structure of coatings and the results of hardness and adhesion with the results of their wear enables a more complete assessment of the possibility of using coatings on tools and machine parts as protective coatings.

II. EXPERIMENTAL

A. *The Coating Preparation*

A set of the VN coatings was deposited using unfiltered cathodic arc evaporation (CAE) in a "Bulat-6" system equipped with a V (99.9 pct) cathode of 60 mm diameter. A vacuum-arc plasma source with magnetic stabilization of a cathode spot was used.[41] HS6-5-2 (DIN standard) steel substrates, 32 mm in diameter and 3 mm thick with the chemical composition (wt pct): C—0.87, W—6.4, Mo—5.0, V—1.9, Cr—4.2, Mn—0.3, Si—0.4 and Fe (balance) were applied. The substrates were finished to a roughness Ra of c.a. 0.02 μm. The process of chemical cleaning of substrates and their mounting on a planetary rotating holder is described in Reference 41. Prior to the coating formation, the pressure in the vacuum chamber was reduced to 2×10^{-3} Pa.

The process of synthesizing V–N coatings consisted of three stages: ion cleaning, deposition at a pressure in a vacuum chamber lower than 1 mPa of a thin (about 0.1 mm thick) adhesive layer of metallic vanadium, improving the adhesion of the V–N coating to the steel substrate, and deposition of the proper V–N coating at the given parameters as in Table I

B. *Coating Characterization Techniques*

The coatings synthesized at various substrate bias voltage and nitrogen pressure were investigated to characterize their thickness, surface morphology, crystalline structure, mechanical properties, as Young's modulus, hardness, adhesion, and tribological properties, *i.e.,* friction and wear. All measurements were performed at least 3 times except X-ray diffraction. A greater number of measurements, 20, were made in the case of hardness (and Young's modulus) tests. The average value of the R_a and R_z coating roughness parameters was calculated from 5 measurements. The friction process was carried out three times under the same conditions. The profile of the wear track (to determine the wear volume) was measured 4 times every 90° for each friction track. The following methods were used to evaluate above mentioned properties, Table II.

The analysis of the friction test parameters presented in the Introduction shows that no higher loads and sliding speeds have been used so far. Therefore, in order to check the behavior of the coatings in severe test conditions, the parameters as in Table II were used.

III. RESULTS

A. *Thickness of the Coatings*

The coatings are characterized by thickness ranging from about 2 μm to about 6 μm. The thickness and other mechanical properties of the coatings strongly depends on both variable technological parameters, nitrogen pressure (Table III) and the substrate bias voltage, Table IV.

Table I. Technological Parameters of VN Coating Synthesize

	Ion Etching	Adhesive Layer	VN Coating	
V Cathode Current (A)	80	80	80	
Argon Pressure (Pa)	0.5	—	—	
			1st set	2nd set
Nitrogen Pressure (Pa)	—	—	0.001 to 3	1.5
Substrate Bias Voltage (V)	− 1300	− 100	− 100	− 50 to − 300
Time (min)	3	3	60	
Temperature,	450 °C	450 °C	450 °C	
Cathode-Substrate Distance (mm)	300	300	300	
Rotation Speed (rpm)	30	30	30	

B. *Chemical Composition of V–N Coatings*

In Figure 1 elemental composition of the coatings deposited in various p_{N2} and [Figure 1(a)] and the U_B [Figure 1(b)] are shown. It can be observed that as the nitrogen pressure increases during the coating deposition, the nitrogen concentration in the coating increases. The coatings, formed under a pressure of not less than 0.5 Pa, are almost stoichiometric and the N/V ratio is approximately 1. The chemical composition of the coating formed at $U_B = -50$ V is 43 at. pct V and 57 at. pct N. With the increase of the negative substrate bias voltage, the V concentration increased almost linearly to 47 at. pct ($U_B = -300$ V). A decrease in the N/V ratio is associated with a simultaneous decrease in nitrogen concentration in the coatings, Figure 1(b).

Presented in Figure 1(b) data indicate that the substrate bias voltage slightly changes the chemical composition of V–N systems deposited using arc evaporation. The tested coatings are not stoichiometric, and the N/V ratio decreases from about 1.3 ($U_B = -50$ V) to about 1.1 ($U_B = -300$ V).

It should be added that a small amount of oxygen, up to about 1.8 at. pct, was recorded in all coatings. It is not an intentional introduction of oxygen into the coating, but an impurity related to the applied method of coating formation—cathodic arc evaporation. Due to its small amount, it was not included in Figure 1.

An increase in the N/V ratio with nitrogen pressure during coating deposition is commonly known.[6,11,13] However, this ratio is presented differently depending on the bias. Qiu *et al.* indicate that it grows and this increase is associated with an increase in ionized nitrogen ions.[13] In turn, Caicedo *et al.* found that the obtained results[8] did not indicate a significant effect of the U_B on the chemical composition of the coatings. They found that at bias from 0 to − 150 V, the atomic percent of N and V was constant. Other results, although only for coatings formed at $U_B = -70$ and − 100 V, are presented in Reference 6. Here, a decrease in the N/V ratio was observed with increasing negative bias.

An almost homogeneous chemical composition is observed [Figure 1(d)] in the cross-section of the coating [Figure 1(c)]. Three zones can be distinguished in Figure 1(d): (I) an increase in the amount of vanadium and oxygen is visible with a simultaneous lower concentration of nitrogen. In zone (II) almost the same concentration of elements is observed in the cross-section of the coating, and in zone (III) the concentration of the coating components decreases and the concentration of iron from the substrate increases. Effects at the boundary of zones (I) and (II) and (II) and (III) may result from the diameter of the electron beam and the analysis of the area above the boundary of the coating—environment or coating—substrate.

C. *The Surface Morphology of V–N Coatings*

The morphology of the surface of the coatings with the highest and the lowest number of surface defects is shown in Figure 2. The coatings were formed at nitrogen pressure of 0.001 Pa [Figure 2(a)] and 0.2 Pa [Figure 2(b)]. The surfaces of other tested coatings had an intermediate amount of surface defects.

Among the many types of defects that may appear on the surface of the coating (nodular—n, red arrows in Figures 2(a), (b), flake, hole/crater—c, yellow arrows, droplet defects—d, blue arrows), the latter most often occur in coatings synthesized using the cathodic arc deposition method. The above defects deteriorate the coating surface quality. Defects in the surface of the coating are the result of the deposition of droplets formed in the arc discharge on it. Droplet defects tend to be more regular in shape than other defects and are usually spherical or oval. They are poorly bonded to the coating. Other defects observed on the surface are discontinuities of the coating—holes or craters of different sizes. Craters are likely formed by the detachment of a droplet defect from the surface of the coating due to stresses in the growing coating.

The roughness parameters R_a and R_z (Table III) are the highest (0.25 ± 0.03 and 2.06 ± 0.23 μm, respectively) for the coating with the highest number of surface defects. The increase in nitrogen pressure in coating deposition results in almost twice decrease in their roughness to the values of 0.13 ± 0.01 and $1.1 \pm 0.1\mu$m, respectively. The coatings synthesized under higher nitrogen pressure are characterized by similar roughness of the coating surface, about 0.18 ± 0.2 and 1.3 ± 0.1 μm, respectively.

The coatings formed with increasing negative substrate bias voltage show slightly decreasing values of roughness parameters, Table IV.

D. *Structure of V–N Coatings*

The coatings formed under a small nitrogen pressure, 0.001 to 0.03 Pa, show only diffraction line (110) from metallic vanadium phase, Figure 3(a). Phase identification was performed according to ICDD card 01-085-4783. Other expected diffraction lines, mainly positioned at 61.2° (200), 77.2° (211) and also the others, were not recorded probably due to their much lower intensity. The coatings synthesized at p_{N2} of 0.07 and 0.2 Pa show apart from (110) V the diffraction line also (211) V line. There is (p_{N2} = 0.03 and 0.07 Pa) also a diffraction line located at about 41.6° coming from the most intense (111) line of V_2N hexagonal phase (ICDD 00-032-1413) or (110) V line. In the coatings synthesized at p_{N2} of 0.2 Pa and above, the presence of the cubic phase of vanadium nitride, c-VN (ICDD 00-035-0768) and also h-VN phase can be observed.

The highest intensity of the diffraction lines was observed for the coating synthesized p_{N2} = 0.5 Pa, and slightly lower for the coating formed at p_{N2} = 0.8 Pa. It is the (001) h-VN phase line (ICDD 01-080-2702).This suggests that these coatings are the best crystallized.

In the coatings formed under a nitrogen pressure ranged from 0.5 Pa to 1.5 Pa, the (001) and (002) h-VN lines are observed, and in a coating synthesized at p_{N2} = 1.5 Pa and 3 Pa also, the most intense (101) diffraction line according to the applied standard, of low intensity here. A (200) diffraction line of the cubic phase of vanadium nitride, c-VN was observed in the coatings formed under nitrogen pressure ranged from 0.8 Pa to 3 Pa. No diffraction lines of (220), (311) and (222) planes parallel to the substrate surface from the c-VN phase were observed. Their strong texturing is indicated by different intensities of diffraction lines characteristic for above phases.

Cubic and hexagonal VN phases of were detected in the coatings synthesized in the previously presented range of substrate bias voltage, Figure 3(b). The coating synthesized with the lowest U_B = − 50 V crystallized in cubic crystal system with space group Fm-3m. In the coatings formed at substrate bias voltage ranged from − 100 to − 200 V the mixture of cubic and hexagonal phases is present. In other coatings from this set of samples only hexagonal phase is observed. On the diffractograms of all samples, except the diffraction lines from the coating, there are also lines from the substrate. It is also worth noting that the determination of substructural characteristics was not carried out for phases with a low content in the sample (due to the weak intensity of the lines or an insufficient number of them). All coatings are strongly textured, the higher the U_B, the more pronounced the texture.

With the increase in nitrogen pressure during the coatings synthesis, the lattice parameter of the pure vanadium cubic phase decreases from 0.3036 nm (p_{N2} = 0.001 Pa) to 0.3012 nm (p_{N2} = 0.2 Pa), while the lattice parameter of the cubic and hexagonal phase of VN increases, Figure 4(a). A similar effect was also reported previously.[11]

The lattice parameter of a cubic VN phase decreases from a = 0.4142 nm at U_B = − 50V to a = 0.4114 nm at U_B = − 200V, Figure 4(b). For hexagonal vanadium nitride, parameter a decreases, and parameter c, on the contrary, increases with U_B increase. The lattice parameter is similar to the value in the above mentioned ICDD cards, which proves the low-stress level in the tested coatings.

The same effect, decrease the lattice parameter from 0.4117 nm for VN coating formed using magnetron sputtering at substrate bias voltage of 0 V to 0.4092 nm for coating formed at substrate bias voltage of − 150 V.[8] Simultaneously, decrease in the lattice constant is accompanied by a reduction in the crystallite size. For coatings formed at the above substrate bias voltages, it was 34 nm and 7 nm, respectively.[8]

The influence of both variable coating synthesis parameters (p_{N2} and U_B) on the crystallite size is also registered, Figures 4(c), (d). With the increase of both above mentioned parameters, a increase in the crystallites of c-VN and their decrease in the h-VN are observed.

E. *Mechanical Properties of V–N Coatings*

The hardness of the coatings synthesized under different nitrogen pressure increases from about 1.5 GPa (p_{N2} = 0.001 Pa) to about 37 GPa (p_{N2} = 0.2 Pa) and then decreases to about 15 GPa (p_{N2} = 3 Pa), Table III. Similar changes are observed for Young's modulus, with the maximum being observed for the coating synthesized under p_{N2} = 1.5 Pa to 570 GPa. With the increase of negative bias, the hardness and Young's modulus of the coatings increase, Table III.

Aissani *et al.* stated, that with increasing nitrogen flow, the hardness of the magnetron sputtered VN coatings increased from approx. 11 GPa to approx. 26 GPa.[11] This is probably due to a change in the stresses in the coating showing the same tendency. A comparable result was presented by Qiu *et al.*[13] An opposite effect was confirmed by Huang *et al.*[10] They showed that with increasing nitrogen flow there was a decrease in hardness from approx. 32 GPa to approx. 30 GPa. This was consistent with a change in compressive stresses in the coatings.

Hardness measurements of a set of coatings synthesized at different substrate bias voltages show an increase in hardness with U_B, as previously reported.[8,13] The opposite effect, a decrease in hardness with U_B, is also observed.[7]

The coating synthesized at p_{N2} = 0.001 Pa is almost pure vanadium (99.9 at. pct) and its hardness is about 1.5 GPa (Table III). For this reason, not all mechanical and tribological properties for this coating were investigated.

The scratch method consists in moving the indenter in two mutually perpendicular directions, horizontally—with constant velocity, and vertically—with rising load. Under the critical load characteristic for the coating-substrate system, the indenter initiates coating cracking, pressing it into the substrate, and finally separating it from the substrate. In this test made it is possible to determine the critical load, *i.e.,* the load at which the delamination of the coatings occurs: the

Table II. Properties of the Coatings—Characteristics of Instruments Applied

Property	Instrument/Type (Manufacturer)	Details
Coating Thickness	calotest	spherical abrasion test method
Surface Profile	contact profilometer/Hommel Tester T8000 (Hommelwerke GmbH, Schwenningen, Germany)	inductive TKL 100 sensor with a diamond stylus tip–tip angle 90° and a nominal tip radius of 1.5 μm tracing length—4.8 mm, tracing speed: 0.15 mm/s, measuring length—4.0 mm, resolution: 0.1 μm
Surface Morphology	scanning electron microscope / JSM-7001F (JEOL Ltd., Tokyo, Japan)	the accelerating voltages was of 10–15 kV
	optical microscope/Nikon Eclipse MA200 (Nikon Corporation, Tokyo, Japan)	magnification objective, low—×1, ×2.5x and top quality high magnification objectives (50x, 100x) were applied
Elemental Composition	scanning electron microscope (JSM-7001F) equipped with EDS (energy dispersive X-ray spectroscopy) microanalyzer JEOL EX-24063 JG (JEOL Ltd., Tokyo, Japan)	the accelerating voltages was of 10–15 kV. The elements were analyzed with an accuracy of approx. 0.5 at. pct (V) and 1.5 at. pct (O)
Phase Composition	X-ray diffractometer/DRON-4-07 (Bourevestnik, Saint Petersburg, Russia)	a Cu-Kα radiation (λ = 0.154056 nm), U = 35 kV and I = 20 mA. Phase analysis—ICDD PDF-2 international database of crystallographic compounds. The analysis was carried out according to the Williamson-Hall method. Annealed silicon-silicon powder was taken as a reference for the selection of instrumental line broadening
Hardness	nano indenter/G200 system (Agilent Technologies, Santa Clara, CA)	the system equipped with Berkovich diamond tip. The continuous stiffness measurement method was used. The average hardness was calculated from ten indentations
Adhesion	Scratch tester/revetest (CSM Instruments, Peseux, Switzerland)	*intender*—diamond C Rockwell type, radius—200 μm Measurements—scratch length—10 mm, indenter speed—10 mm/min, loading force increase 0 to 200 N *number of scratches*—at least three *critical loads*—Lc1—the first damage to the coating appears, from the curve of acoustic emission as a function of normal load recorded during testing and microscopic observations, Lc2—complete delamination of the coating, determined from microscopic observations
	Daimler–Benz test	the Baimler -Benz test was performed by applying a force of 1471N to the coating. It is a qualitative destructive test for coating / sub strate systems. In this test, damage to the layer adjacent to the Rockwell indentation boundary is observed and compared with a defined pattern of adhesion force.[42]
Friction and Wear	ball on disc / T-01 M (Institute for Sustainable Technologies, Radom, Poland)	*counterpart*—Al_2O_3 ball, 10 mm in diameter, hardness of 15 GPa and Ra < 0.03 μm *test conditions*—normal load 20 N, sliding distance of 2000 m, sliding speed 0.2 m/s, sliding radius—12 mm, dry sliding, ambient temperature, humidity around 50 pct

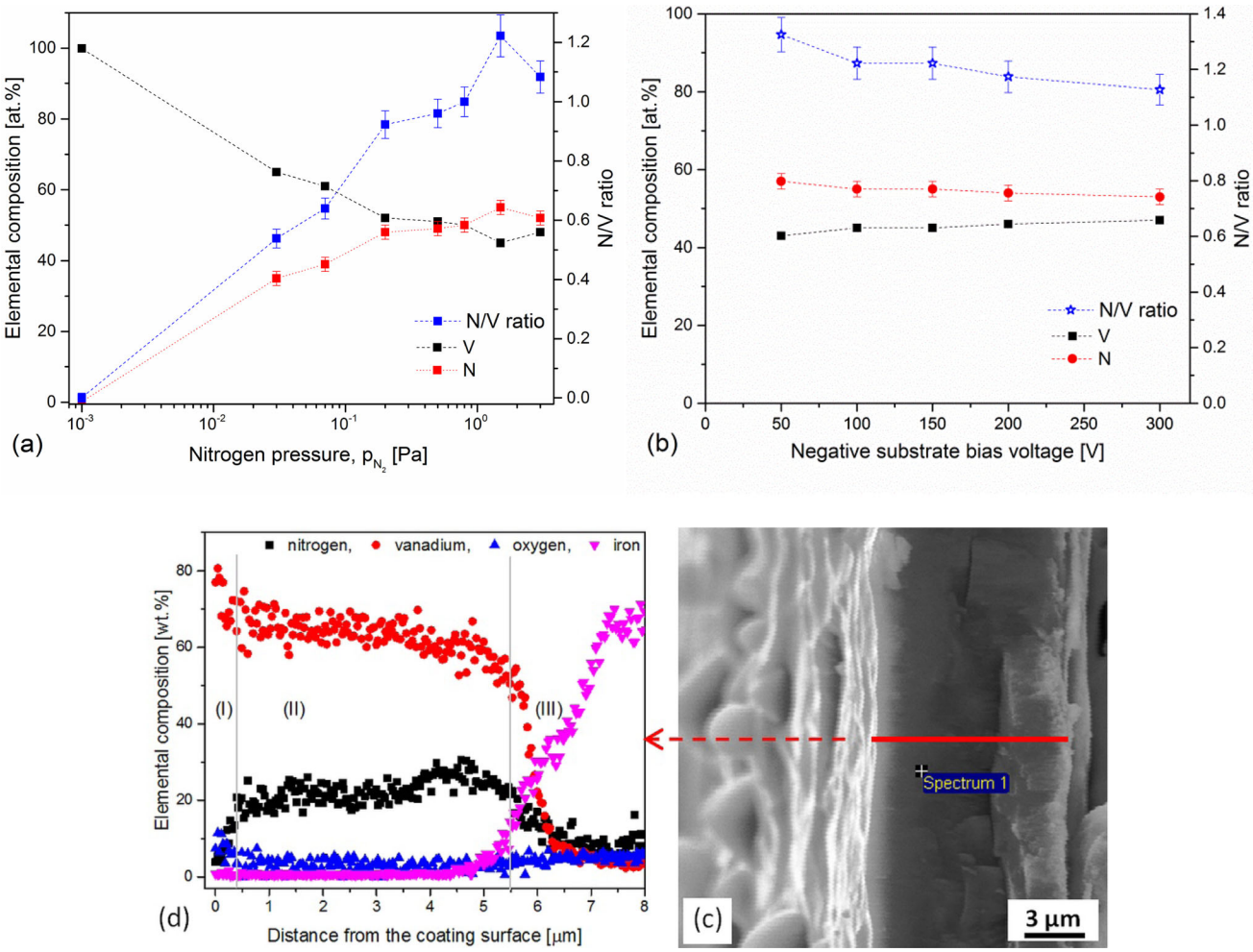

Fig. 1—Elemental composition of the V–N coatings deposited under different (*a*) p_{N2} and (*b*) - U_B. The cross-section of the coating deposited under nitrogen pressure of 1.5 Pa and substrate bias voltage of − 100 V (*c*) and the EDS analysis in the cross-section (*d*). Dotted lines in this and other figures are only for eye guiding.

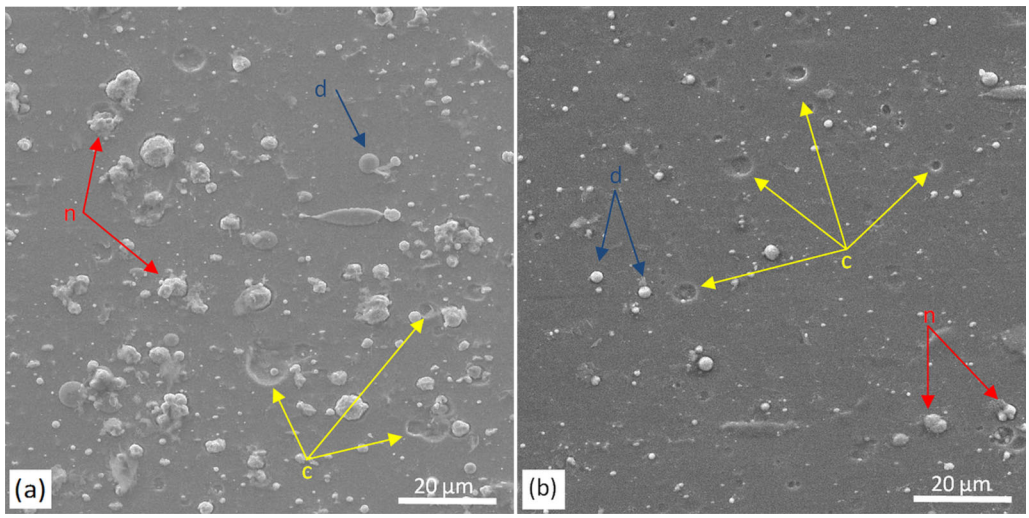

Fig. 2—SEM pictures of the V–N coatings formed under p_{N2}: (*a*) 0.001 Pa, (*b*) 0.2 Pa.

Table III. Characteristics of V–N Coatings Formed Under Various Nitrogen Pressure

Parameter	Nitrogen Pressure, p_{N2} [Pa]			
	0.001	0.03	0.07	0.2
Thickness (μm)	2.0 ± 0.2	2.5 ± 0.2	3.0 ± 0.2	3.5 ± 0.2
Roughness R_a (μm)	0.25 ± 0.03	015 ± 0.02	0.16 ± 0.03	0.13 ± 0.01
Roughness R_z (μm)	2.06 ± 0.23	1.14 ± 0.22	1.35 ± 0.42	1.09 ± 0.11
Hardness	1.5 ± 0.3	27.7 ± 1.5	32.2 ± 2.2	37.3 ± 2.1
Elastic Modulus	70 ± 8	328 ± 21	387 ± 23	522 ± 26
Critical Load (N)	—	70 ± 15	66 ± 13	87 ± 4
Wear Rate, × 10^{-7} (mm^3/Nm)	132 ± 32	17.0 ± 2.1	7.2 ± 1.1	1.3 ± 0.2
Parameter	Nitrogen Pressure, p_{N2} [Pa]			
	0.5	0.8	1.5	3.0
Thickness (μm)	3.7 ± 0.3	4.0 ± 0.3	5.7 ± 0.4	4.7 ± 0.4
Roughness R_a (μm)	0.19 ± 0.02	0.17 ± 0.02	0.18 ± 0.03	0.18 ± 0.02
Roughness R_z (μm)	1.31 ± 0.06	1.43 ± 0.06	1.19 ± 0.07	1.31 ± 0.18
Hardness	36.4 ± 2.5	34.8 ± 1.8	29.0 ± 1.5	15.6 ± 1.2
Elastic Modulus	537 ± 29	516 ± 33	570 ± 30	365 ± 24
Critical Load (N)	92 ± 5	80 ± 1	113 ± 2	146 ± 3
Wear Rate, × 10^{-7} (mm^3/Nm)	1.2 ± 0.3	0.6 ± 0.4	1.3 ± 0.3	1.5 ± 0.4

coatings synthesized at various p_{N2} (Table III) or U_B, Table IV. It can be seen that the adhesion of the coatings increases almost linearly from about 70 N (p_{N2} = 0.03 Pa) to about 140 N (p_{N2} = 3 Pa) with nitrogen pressure. The coatings synthesized at various substrate bias voltage have a more complex dependence on U_B. The lowest Lc_2 value is characteristic for coatings synthesized at U_B = − 150 V, about 100 N. At other voltages they show higher adhesion—about 150 N (U_B = − 50 V) and about 120 N (U_B = − 300 V).

The same test on the V_2N and VN coatings showed significantly higher critical load Lc_2 for VN coating—about 130 N than V_2N—about 80 N.[27] Critical load Lc_1 corresponding to the cohesive failure for the above coatings are slightly lower, about 10 pct. The much lower Lc_1 critical load for the VN (63 N) coating is presented in Reference 17.

In Figure 5 a big difference in critical loads and coating failures of selected coatings is presented. It is worth pointing out that the value of the critical load (30, 60 N, *etc.*) presented in Figure 110 refers to the center of the fragment of the appropriate scratch, and the width of the scratch image corresponds to the difference in critical loads equal to 2 N. With a load of 30 N, the scratch after passing the indenter is hardly visible. All coatings are not damaged. At a load of 60 N, conformal cracking[43] is visible in the coating formed at 0.2 Pa, when coating try to conform to the groove. Above damages are open away from the direction of scratch. The other coatings are characterized by a rather smooth scratch bottom. One can also notice small chipping on the edge of the scratch. Cohesive failures of the coatings occur at a load between 30 N and 60 N. Increasing the normal load results in more severe damage to the coating, its cracking and chipping, especially at the scratch boundaries, and leads to the coating delamination.

The coatings are characterized by good adhesion with a critical load of above 66 N, Table III and IV. Another quick method for evaluating coating adhesion is the Rockwell test in which both coating brittleness, cohesion as well as the interfacial adhesion is exhibited. The microscopic image of the type of cracks in the coating and its delamination at the indentation boundaries are analyzed. The coating adhesion is then assigned to one of the six adhesion classes. The best adhesion is demonstrated for coatings showing only radial cracks of the coating at the edges of the indentation and the presence of no more than a small local delamination of the coating.

All tested coatings synthesized under variable nitrogen pressure (Figure 6) and the substrate bias voltage (Figure 7) show acceptable failures and can be classified as HF1. Figure 6 shows the failures of the coatings synthesized at p_{N2} of 0.03 Pa, 0.07 Pa, 0.5 and 3 Pa, *i.e.,* characterized by the lowest [Lc_2 = (66 ± 13) N, p_{N2} = 0.07 Pa, Figure 6(b)] and the highest (Lc_2 = (146 ± 3) N, p_{N2} = 3 Pa, Figure 6(d) adhesion. The coatings synthesized under the other pressures showed slight radial cracks as in Figures 6(c), (d).

The coatings synthesized at various substrate bias voltages have a critical load above approx. 100 N. The highest load is shown by the coating formed at U_B = − 50 V, about 147 N [Figure 7(a)], while the lowest—about 97 N, the coating formed at U_B = − 150 V, Figure 7(b). A critical load of other coatings is about 110 to 120 N.

F. *Tribological Properties of V–N Coatings*

Figure 8 shows examples of friction coefficient changes over time, and in the tables inside, a list of

Table IV. Characteristics of V–N Coatings Formed Under Various Substrate Bias Voltage

	Substrate Bias Voltage, U_B [V]				
Parameter	− 50	− 100	− 150	− 200	− 300
Thickness (μm)	5.7 ± 0.4	5.7 ± 0.4	5.2 ± 0.4	5 ± 0.4	3.8 ± 0.3
Roughness R_a (μm)	0.19 ± 0.04	0.18 ± 0.03	0.18 ± 0.01	0.13 ± 0.01	0.18 ± 0.02
Roughness R_z (μm)	1.45 ± 0.40	1.19 ± 0.07	1.32 ± 0.09	1.22 ± 0.35	1.31 ± 0.12
Hardness	20.2 ± 1.5	29.1 ± 2.2	35.9 ± 1.9	37.2 ± 2.0	35.7 ± 2.3
Elastic Modulus	391 ± 33	570 ± 30	523 ± 22	510 ± 35	492 ± 38
Critical Load (N)	147 ± 4	113 ± 2	97 ± 9	114 ± 3	121 ± 6
Wear Rate, × 10^{-7} (mm^3/Nm)	5.7 ± 0.3	1.3 ± 0.3	0.8 ± 0.3	0.8 ± 0.2	0.5 ± 0.2

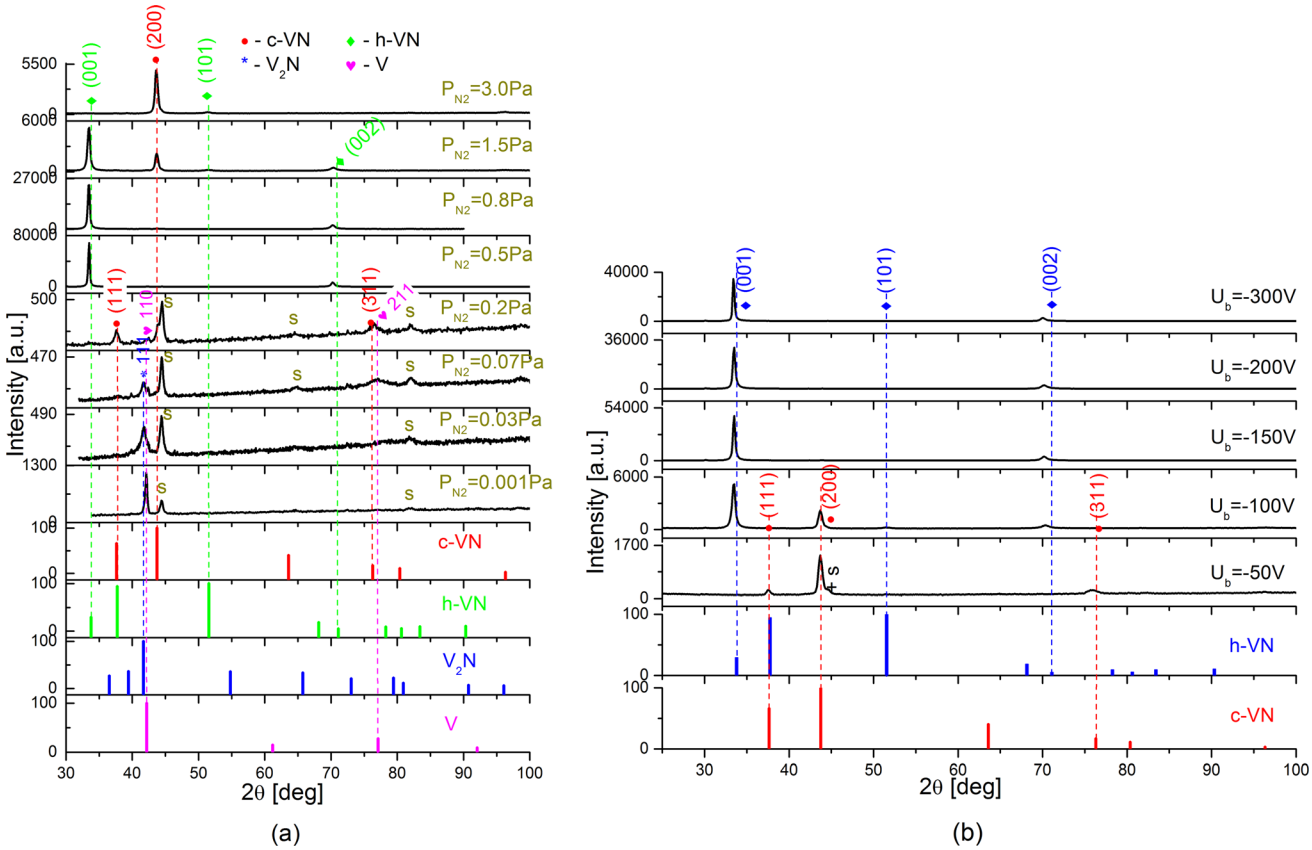

Fig. 3—XRD patterns of the V–N coatings synthesized under different (*a*) p_{N2} and (*b*) U_B. Symbol "s" in both figures means substrate.

calculated friction coefficients for coatings formed at different nitrogen pressure [Figure 8(a)] and substrate bias voltage [Figure 8(b)].

Relatively high values of friction coefficient from 0.51 to 0.66 were recorded for V–N coatings synthesized at nitrogen pressure from 0.03 Pa to 3 Pa, Figure 8(a). A slight decrease in the friction coefficient with increasing nitrogen pressure can be noticed. The slope of the least squares line is about − 0.05.

For coatings synthesized at different substrate bias voltages the values of the coefficient of friction are similar. However the nature of their changes is different. The friction coefficient increases almost linearly from 0.56 (U_B = − 50 V) to 0.67 (U_B = − 150 V) and then decreases to 0.48 (U_B = − 300 V), Figure 8(b).

In Table III and IV are summarized the wear rates (kv) for all coatings calculated as the volume of coating material removed from the friction track during the ball-and-disk test divided by the product of the length of the sliding distance and the normal load. With increasing nitrogen pressure in deposition process, the wear rate of the VN coatings decreased. The coating formed at a pressure of 0.001 Pa with a metallic vanadium structure (Table III) is characterized by a high wear rate, about 3.2 × 10^{-5} mm^3/Nm. This rate is much lower for

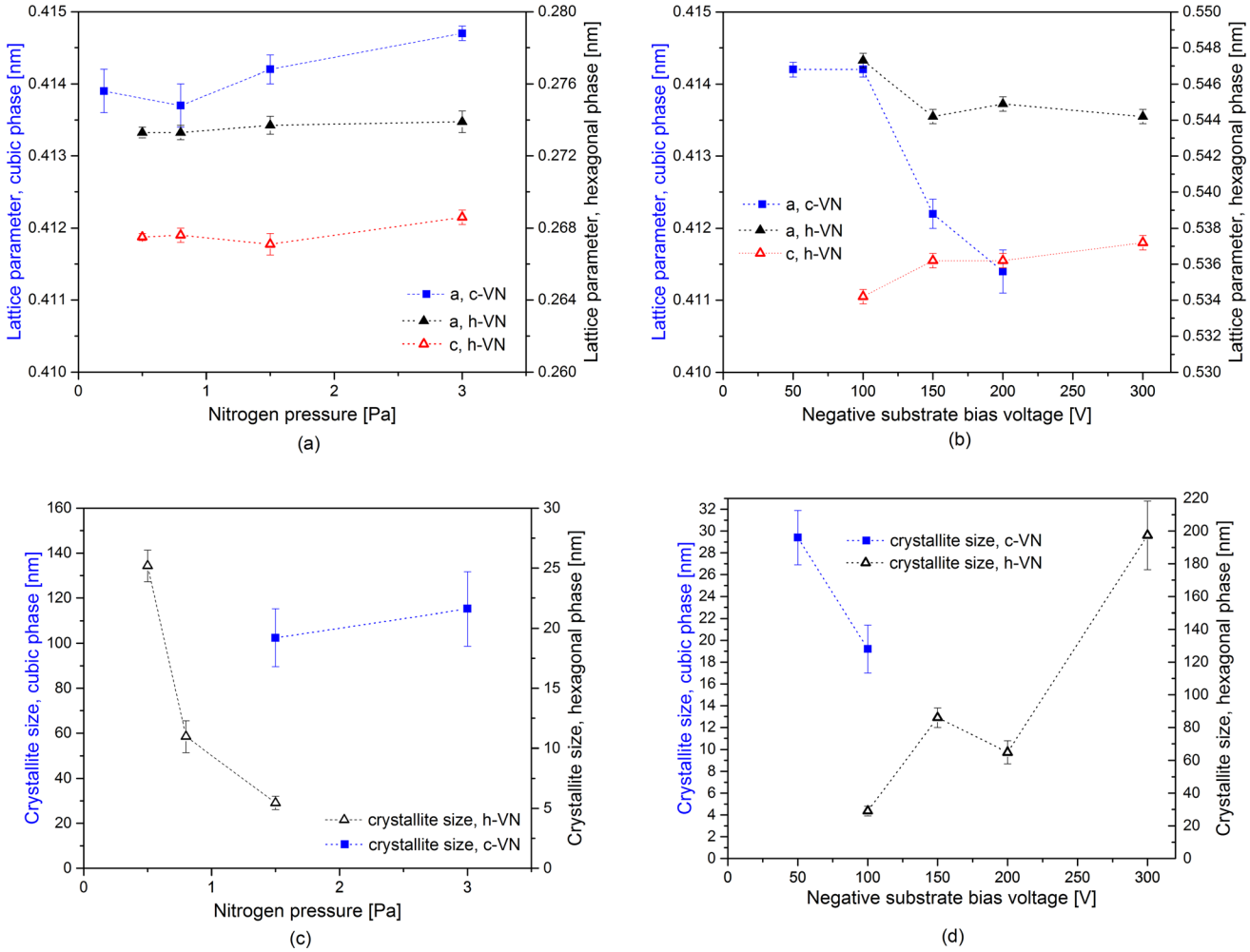

Fig. 4—Lattice parameter (*a*, *b*) and crystallite size (*c*, *d*) of the V–N coatings synthesized under different p_{N2} (a, c) and U_B (b, d).

the coatings formed with nitrogen pressure not lower than 0.2 Pa - below 1.4×10^{-7} mm^3/Nm, Table III. This means that the coatings synthesized at higher p_{N2}, where the N/V ratio is close to 1 or higher, are characterized by better wear resistance.

The coatings synthesized at various substrate bias voltages are characterized by lower wear rate. For the coating formed at substrate bias voltage of − 50 V, it is the largest and amounts to approximately 5.7×10^{-7} mm^3/Nm, and decreases to about 4.9×10^{-8} mm^3/Nm (Table IV) with the increase of negative substrate bias voltage.

A comparison of the same coatings produced using cathodic arc evaporation and magnetron sputtering indicates a higher wear resistance of the former. Aissani *et al.*[11] reported that the lowest value of the wear rate (2.72×10^{-5} mm^3/Nm) was observed for the coating formed in Ar + N_2 mixture at nitrogen flow rate of 20 sccm, corresponding to ratio of N/V = 1. The coatings formed at lower and higher nitrogen flow rates were characterized by a higher wear rate - worse wear resistance. They also showed the dependence of the wear rate on the coating thickness, the wear rate decreasing with increasing coating thickness.[12] Similarly, the coating formed using cathodic arc ion plating technique with the ratio of N/V = 0.86 had a wear rate of about 3×10^{-6} mm^3/Nm and a friction coefficient against Al_2O_3 ball of 0.68.[44] Similar results of the wear rate and coefficient of friction were shown for the V(C)N coatings by Cai *et al.* [217].

Similar coatings, formed by cathodic arc evaporation, tested under the conditions presented in this work (normal load 20 N, sliding speed 0.2 m/s and sliding distance 1000 to 2000 m) had lower wear rates. For CrN it ranged from 1×10^{-6} mm^3/Nm to 2×10^{-7} mm^3/Nm depending on the concentration of nitrogen in the coating,[45] while for Cr- V–N it decreased from 4.1×10^{-6} mm^3/Nm (CrN) to 1.2×10^{-7} mm^3/Nm.[40]

However, significantly lower values for the wear rate are also shown. The coatings deposited by magnetron sputtering, tested in the reciprocating ball-on-disc with Al_2O_3 ball as a counterpart, under the sliding speed and normal load of 0.05 m/s and of 5 N, respectively, showed a wear rate of about 3×10^{-8} mm^3/Nm.[37]

In Figure 9 are presented selected wear tracks of investigated coatings formed under different nitrogen pressures. There is a noticeable reduction in the wear track width. The coating synthesized at p_{N2} = 0.03 Pa

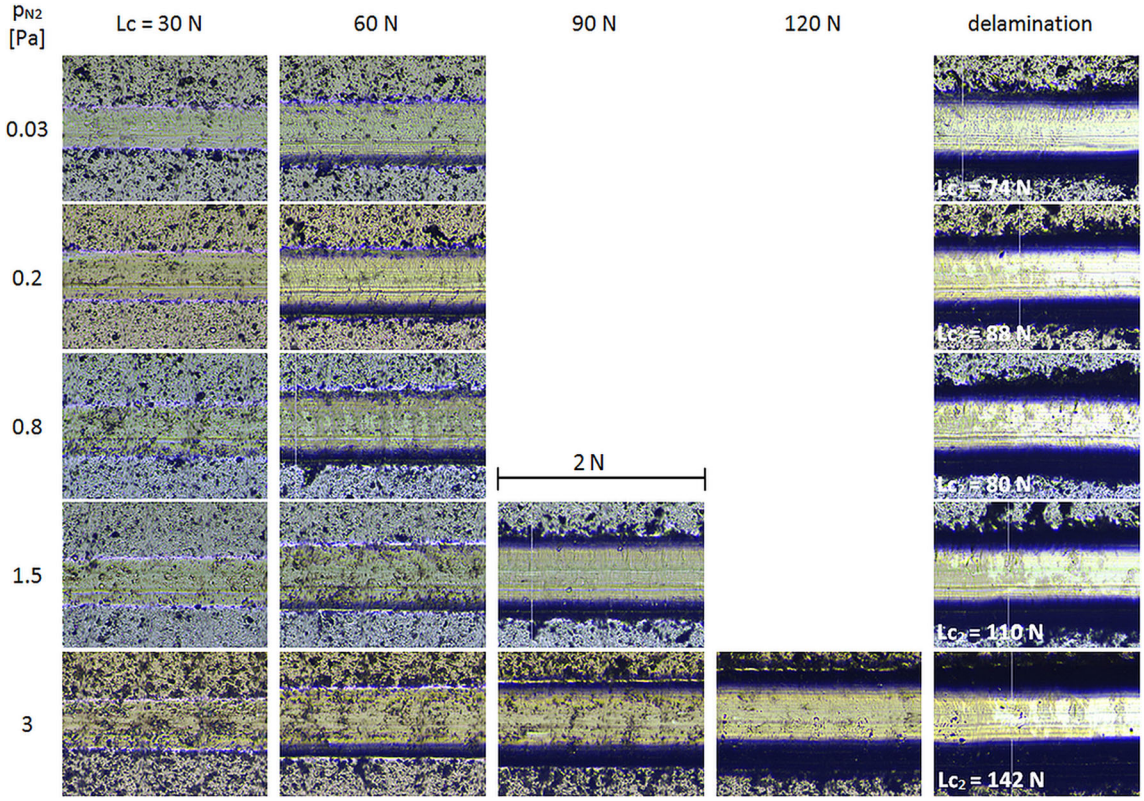

Fig. 5—The view of scratches from scratch test of the V–N coatings synthesized under various nitrogen pressure p_{N2}.

is characterized by maximum wear track depth (about 2.1 μm) and width (about 780 μm), which indicates high abrasive wear. The coatings synthesized at higher nitrogen pressures are characterized by a smaller wear track width and depth. Only small abrasive wear is observed, Figures 9(b) through (d). No wear debris was observed at the edges of the tracks. For the coating synthesized at p_{N2} = 0.2 Pa [Figure 9(b)], the wear track width and depth are approximately 542 and 0.38 μm, respectively, and decrease to approximately 480 and 0.26 μm for the coating synthesized at p_{N2} = 3 Pa, Figure 9(d). The smallest width (about 430 μm) was found for the coating synthesized under p_{N2} = 0.8 Pa. It also shows the smallest wear depth - about 0.22 μm, Figure 9(c). This coating is characterized by the lowest wear rate, $(6.2 \pm 0.5) \times 10^{-8}$ mm^3/Nm (Table III).

Small wear track depths for the coatings formed under $p_{N2} > 0.2$ Pa means that with increasing in N/V ratio in the coatings increases their wear resistance. The wear tracks of the above coatings are smooth without debris, which indicates their better tribological performance.

Figure 10 shows two images of friction tracks in the coatings from the set formed at different substrate bias voltage, with the lowest bias, $U_B = -50$ V [Figure 10(a)] and the highest $U_B = -300$ V [Figure 10(b)]. The wear tracks of the other coatings from mentioned set are similar to the image shown in Figure 10(b). Among the set of coatings formed at different substrate bias voltage, the coating formed at $U_B = -50$ V has the largest width, about 544 μm and a wear track depth - about 1.0 μm. High abrasive wear of the coating is visible. The same abrasive mechanism is likely to occur as for the coating synthesized at p_{N2} = 0.03 Pa.

The coating formed at $U_B = -100$ V has a width of about 510 μm and a significantly smaller wear track depth, about 0.20 μm. The wear track width decreases almost monotonically to about 420 μm ($U_B = -300$ V) with negative substrate bias voltage increase. The change in the wear track depth has a similar character. For the recently presented coating it amounts to about 0.12 μm.

In Figure 11 are presented the SEM surface of the coating at two magnifications [Figures 11(a), (b)] and the results of the elemental analysis of the surface [Figure 11(c)], as well as SEM images of the wear track [Figure 11(d)] and its bottom [Figure 11(e)] and the EDS results [Figure 11(f)] of the bright area, white rectangle in [Figure 11(e)]. The smooth bottom of the path is visible with craters from poorly bonded macroparticles removed from the coating surface in friction test. There is also a significant difference in oxygen concentration in the coating and in the friction track. The N/V ratio in both cases [Figures 11(c), (f)] is similar and amounts to about 1.08.

The wear rate of the Al_2O_3 counterpart is about one or two levels lower than that of the tested coatings. As can be seen in Figure 12, where images of abrasion of several counterparts are shown, the largest diameter of abrasion is shown by the ball cooperating with the coating synthesized under a pressure of 0.03 Pa, about 850 μm.

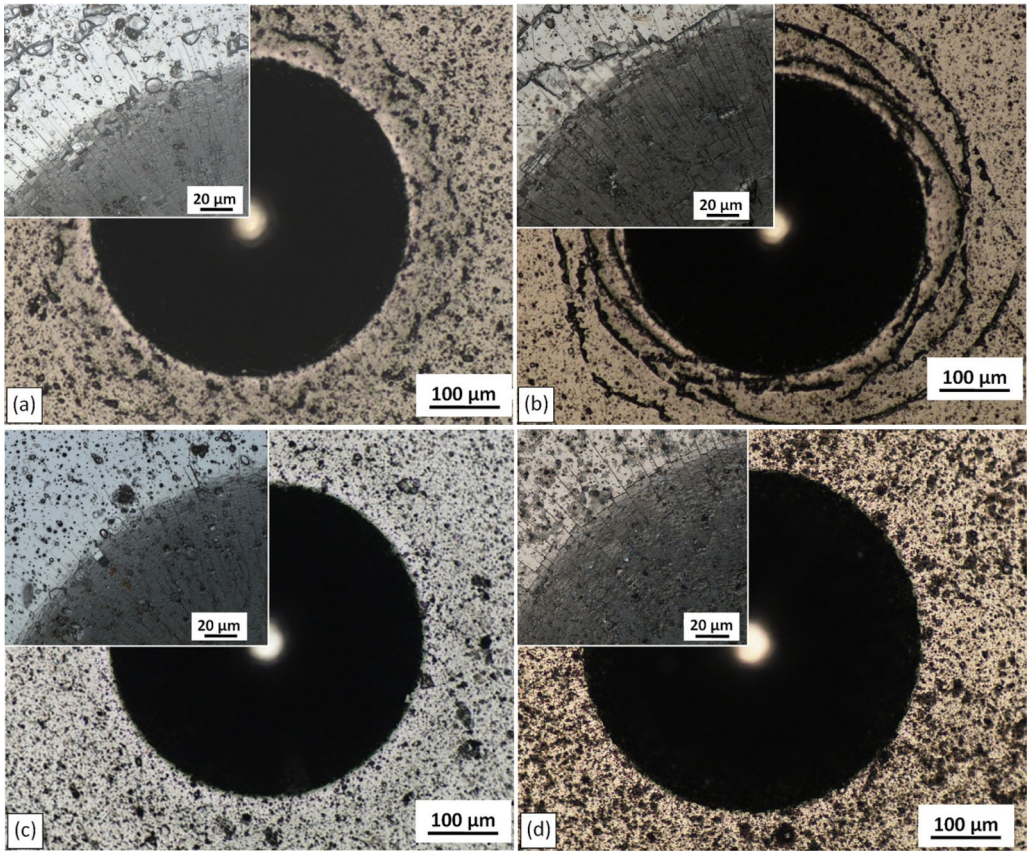

Fig. 6—Rockwell indentation images of the V–N coatings synthesized at p_{N2} of: (*a*) 0.03 Pa, (*b*) 0.07 Pa, (*c*) 0.5 Pa, (*d*) 3 Pa.

This corresponds to a ball wear rate (kb) of approx. 6.6×10^{-8} mm^3/Nm. The wear rate of this coating is 1.7×10^{-6} mm^3/Nm. For coatings synthesized at higher nitrogen pressure, the counterpart abrasion diameter is smaller, as well as the wear rate is lower for them. For a coating formed under a pressure of 0.8 Pa, the ball abrasion diameter is about 630 μm (kb = 1.9×10^{-8} mm^3/Nm, kv = 6.2×10^{-8} mm^3/Nm). A slightly larger ball wear diameter (about 640 μm) was observed after the test with a coating synthesized under a pressure of 3 Pa. It is characterized by a slightly higher coating wear rate (approx. 1.5×10^{-7} mm^3/Nm) than the previously described one. It was observed that the lower the wear rate, the smaller the wear diameter of the counterparts.

IV. DISCUSSION

A. *Effect of Nitrogen Pressure*

With increasing nitrogen pressure, the number of ions involved in the coating formation process increases. As a result, the thickness of the coating increases, and due to the constant time of their formation, the deposition rate. However, as nitrogen pressure increases, the number of collisions increases, which can reduce the kinetic energy of the particles, their velocity and free path. As a result, the deposition rate may decrease. Another phenomenon is ''target poisoning''. Higher melting point of vanadium nitride synthesized on the cathode surface (2050 °C) than of the vanadium cathode (1910 °C) may reduce the deposition rate of the VN coatings.

The results of many studies confirm the decrease in the deposition rate of V–N coatings with nitrogen pressure increase.[10,11,13,14] This may be related to a decrease in the target sputtering rate as a result of ''target poisoning''.[13,14]

What is important, however, is the atmosphere in which the coating is deposited. The findings of Zhang *et al.*[46] indicate higher sputtering capability of argon compared to nitrogen. This means that the deposition rate of the coating synthesized from the vanadium cathode in an atmosphere of a mixture of nitrogen and argon is completely different than in a pure nitrogen atmosphere. Thus, the deposition rate of the coatings formed in the Ar + N_2 atmosphere will decrease with increasing nitrogen content in this mixture of gases.

The analysis of the above phenomena shows that in the case of the coating formation in a nitrogen atmosphere, the increase in the deposition rate results from an increase in its pressure. The increase in collisions of gas atoms causes a decrease in their kinetic energy. Resputtering efficiency drops, which causes an increase in the deposition rate. Similar effect was observed, for example, in CrN[47] and CrAlN.[23]

The surface quality of the coating and its morphological features are influenced by two factors: the quality of the substrate preparation and the method of the

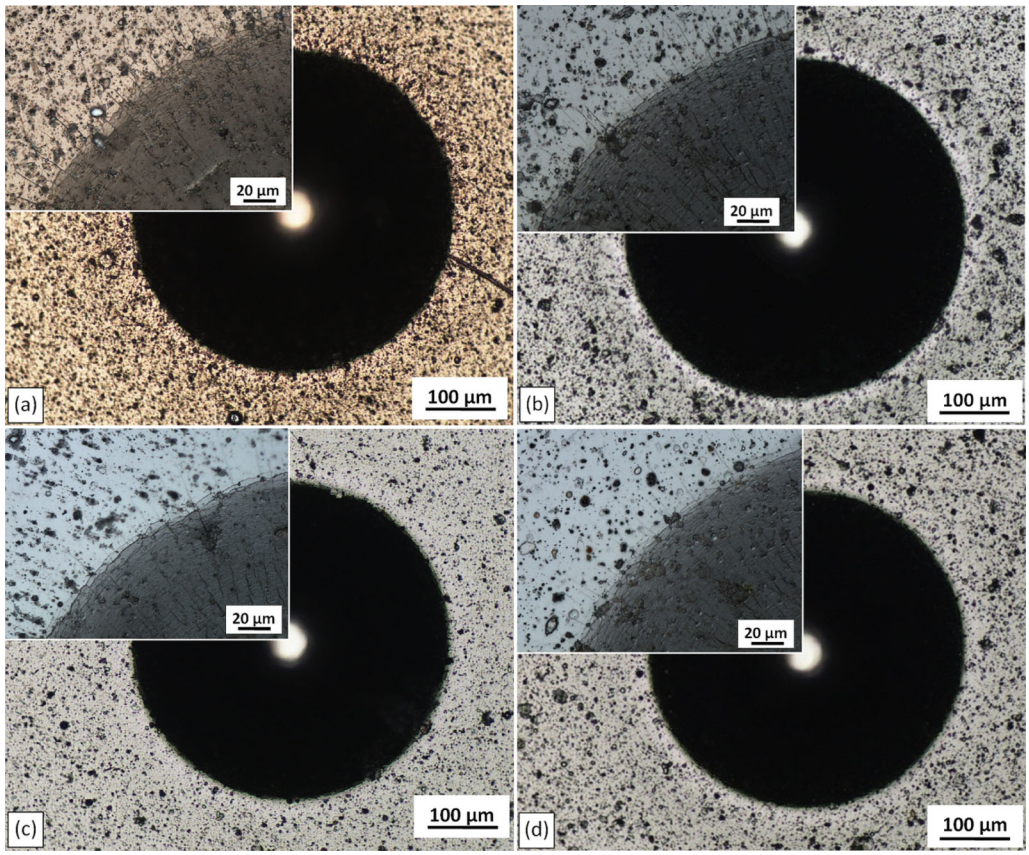

Fig. 7—Rockwell indentation images of the V–N coatings synthesized at U_B: (*a*) − 50 V, (*b*) − 150 V, (*c*) − 200 V, (*d*) − 300 V.

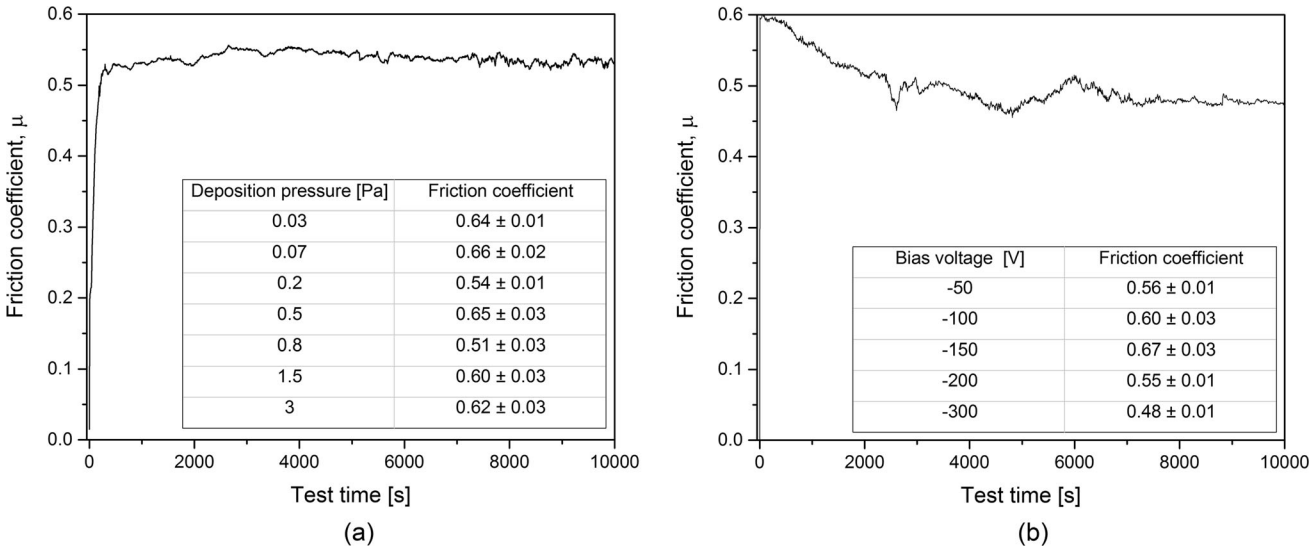

Fig. 8.—Dependence of friction coefficient on test time of the V–N coatings synthesized under nitrogen pressure of 0.2 Pa (*a*) and substrate bias voltage of − 300 V (*b*). Inside, tables with friction coefficients of coatings formed in various p_{N2} and U_B.

coating formation. The morphological features of the substrate are reflected on the coating surface, usually this effect is magnified.[48] Therefore, all substrates were mechanically prepared and ion-cleaned in the same manner and under the same conditions. The purpose of these treatments was elimination of irregularities and fine particles from the substrate surface that could result in coating growth defects due to the shadowing effect. The method of the coating deposition also demonstrates a significant impact on the quality of its surface. The coatings formed by the magnetron sputtering method are characterized by much smaller number of surface

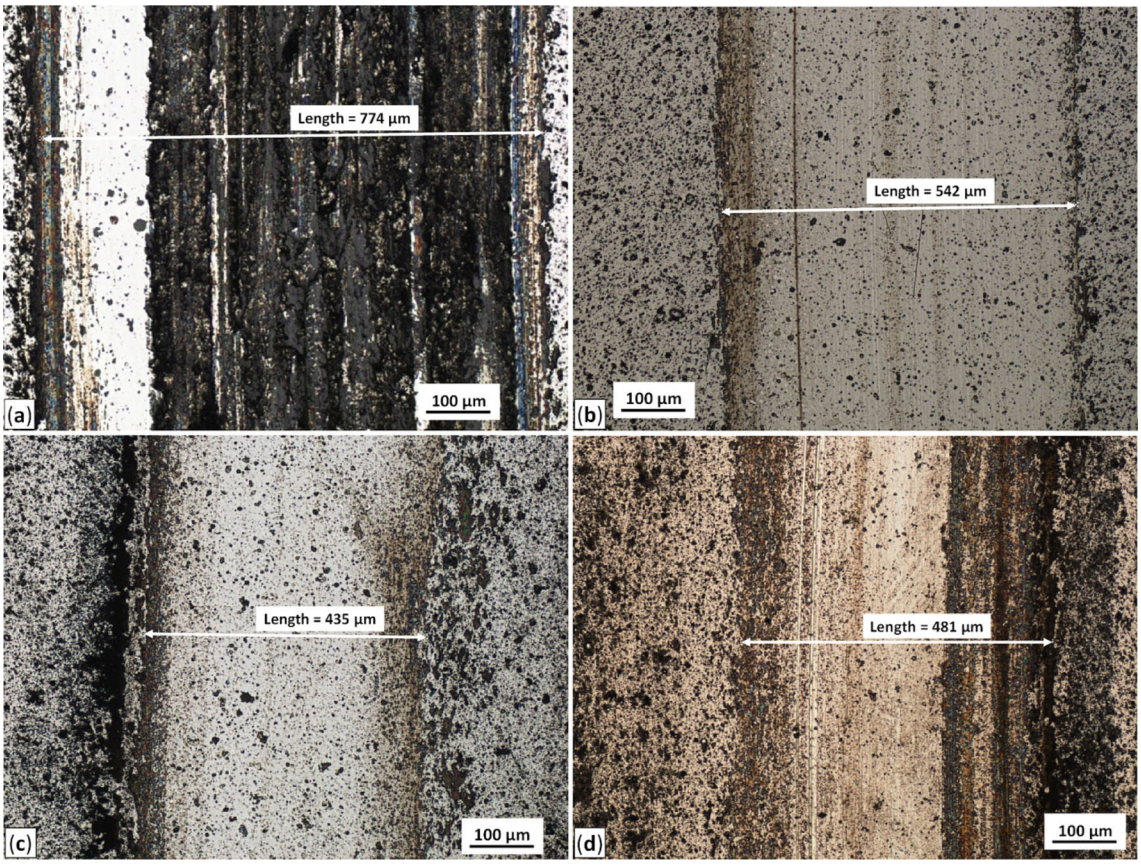

Fig. 9—Optical microscopy images of the V–N coatings synthesized at nitrogen pressure: (*a*) 0.03 Pa, (*b*) 0.2 Pa, (*c*) 0.8 Pa, (*d*) 3 Pa.

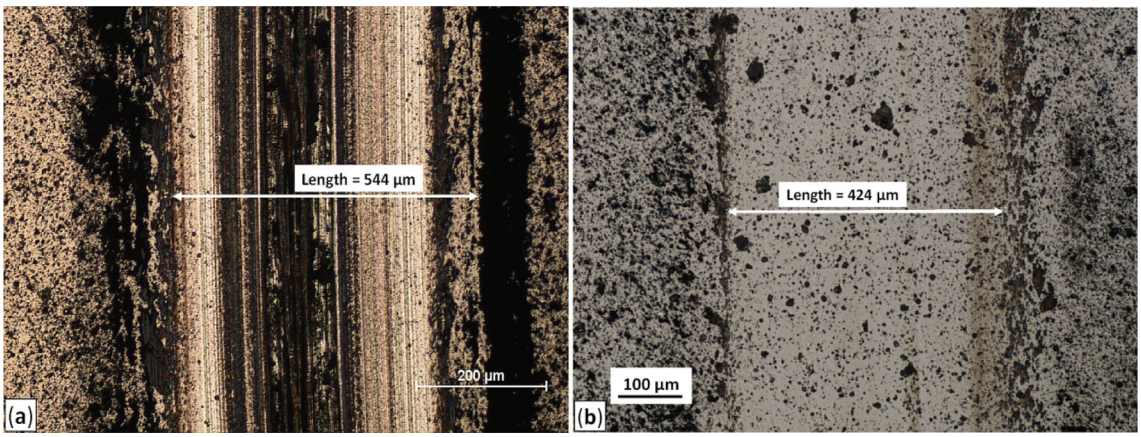

Fig. 10—Optical microscopy images of the V–N coatings synthesized under substrate bias voltage of: (*a*) − 50 V, (*b*) − 300 V.

defects than those synthesized by cathodic arc evaporation.[48,48] It should be noted that the cathodic arc evaporation deposition method is characterized by a large number of defects such as nodular, flake, hole/crater, droplet defects and others. In general, they worsen the surface roughness of the coating, cause pores as a result of the removal of droplets by high compressive stresses in the coating, and may contribute to local loss of its adhesion. However, the number of surface defects can be reduced by reducing the arc current (which leads to a lower deposition rate and extending the time of the coating deposition process), increasing the partial pressure of the reactive gas during deposition (see Table III) or increasing the substrate bias voltage (see Table IV), which results in increased re-sputtering. No flake defects were observed, which may indicate good adhesion of the coatings to the substrate.

The phase transformation of the coatings related to the increasing nitrogen pressure during their formation is quite complex. At low pressure of nitrogen, only the

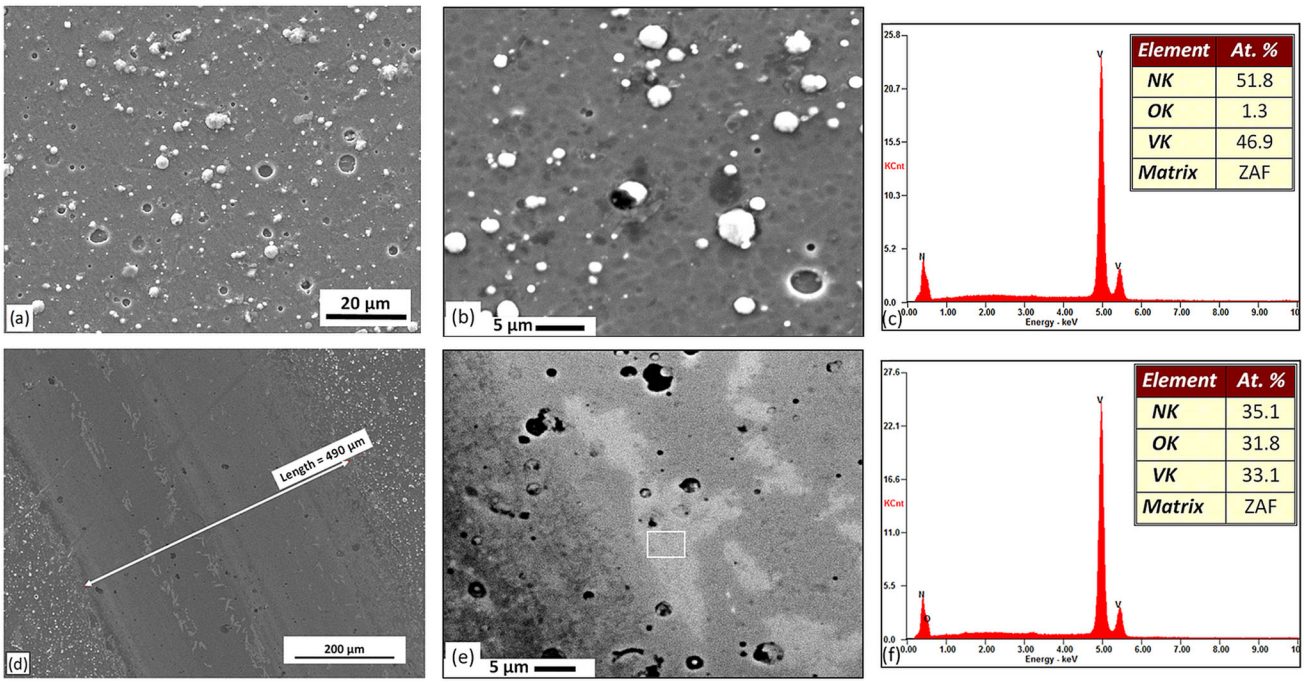

Fig. 11—SEM images of the coating ($_{pN2}$ = 1.5 Pa, U_B = − 100 V) surface in different magnification (a, *b*), the EDS results of the surface (*c*), SEM images of the wear track (*d*) and its bottom (*e*) and the EDS results (*f*) of the white area, white rectangle in (e).

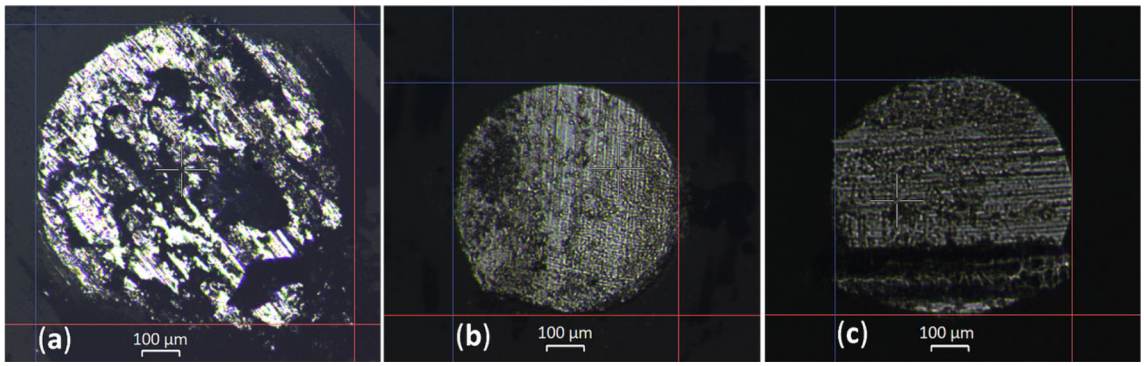

Fig. 12—Abrasion of the Al_2O_3 ball counterpart after a dry sliding wear test against V–N coatings synthesized at nitrogen pressure: (*a*) 0.03 Pa; (*b*) 0.8 Pa; (*c*) 3 Pa.

vanadium V phase synthesizes. In the shells synthesized at $p_{N2} > 0.03$ Pa, apart from the V phase, the addition of the V_2N phase, and then the cubic c-VN phase is observed. At a nitrogen pressure above 0.5 Pa, highly textured coatings are formed consisting of VN phases: hexagonal h-VN and cubic c-VN. At p_{N2} = 0.5 Pa, h-VN nitride is formed, above this pressure, a decrease in the amount of h-VN nitride in the coatings and a corresponding increase in the content of c-VN nitride are observed. Based on diffractograms of the coatings synthesized under different nitrogen pressure [Figure 3(a)], the diagram of structure evolution can be shown , Figure 13.

The lattice parameters increase of VN-h and VN-c nitrides is also observed with increasing the nitrogen pressure during coating synthesis, Figure 6(a). This may be due to the higher nitrogen concentration in the coating, Figure 2(a), resulting in the observed increase in microstress.

Figures 1(a) and 4(c) show that the crystallite size decreases with the increase of the N/V ratio. According to the Hall-Petch relationship, this may be responsible for the observed increase in hardness, Table III. The increase in the lattice parameter with the N/V ratio observed here is confirmed by previous studies of coatings formed by magnetron sputtering.[11,16]

The hardness of the material depends on many factors, including the V–N ionic binding energy, the ordering of the structure, the additives present in the structure and their amount, microstructure and porosity. It was previously reported that TiN coatings with (111) crystal plane show the highest hardness.[50] It seems that because V–N coatings are characterized by the space group number (225) and similar lattice

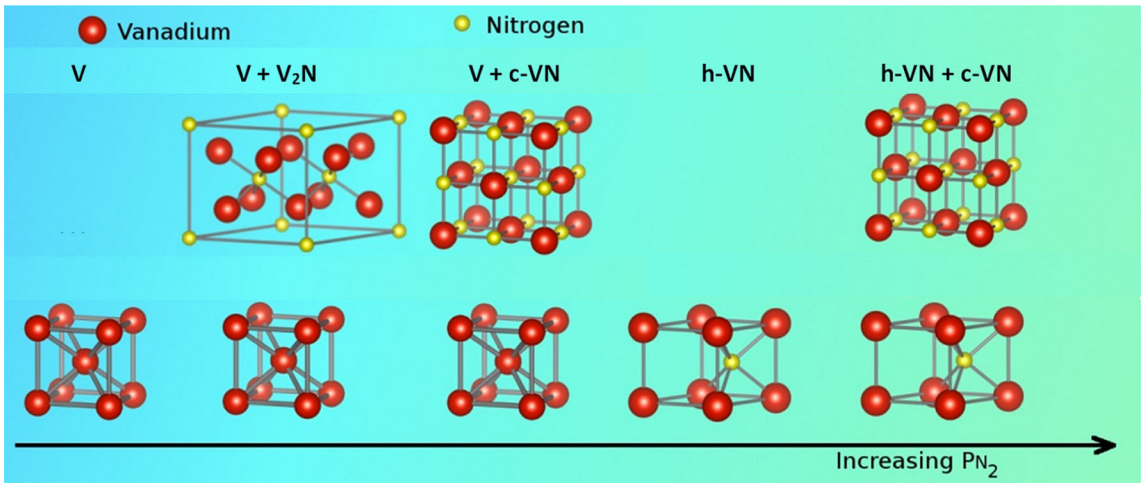

Fig. 13—Structure evolution of the V–N coatings with nitrogen increase.

parameter one can expect similar behavior. As can be seen in Figure 3(a), the (111) VN diffraction line is visible in the coating formed under the pressure of 0.2 Pa. This coating is characterized by the highest hardness among coatings formed under pressure in the range of 0.001 Pa to 3 Pa, Table III.

The high values of the critical force Lc_2 are related to the used Rockwell C indenter with a diamond tip radius of 200 μm and the type of substrate on which the coating was synthesized. One of the findings of Valleti *et al.*[51] was to determine the relationship between substrate hardness and adhesion. They found that the higher the hardness of the substrate, the higher the adhesion of the coatings. Here, the coatings were deposited on heat-treated HS6-5-2 steel substrates.

The friction coefficient of VN coating synthesized at pressure of nitrogen below 0.1 Pa is high, Figure 8(a). Such a high value is probably related to the hexagonal V_2N phase presence in the coating.

In the initial sliding stage [friction curve in Figure 8(a)], a low value of the friction coefficient is observed, which then quickly increases to a constant level after about 250 s of the test, *i.e.,* 50 m of the sliding distance. Surface roughness plays an important role in this running-in stage. Coatings with high roughness, in which the contact surface of the coating with the counterpart is small (running-in stage, are characterized by a low coefficient of friction,[11] which increases as the surface defects (macroparticles) are removed and the contact area of the coating with the counterpart increases.

It should also be added that no detachment of the coating from the substrate was observed in the wear track for any of the observed coatings. The test parameters, especially the sliding distance, were selected so that the wear depth was not greater than the thickness of the coating. It is known that friction coefficients of coating-counterpart and substrate-counterpart systems differ significantly. As can be seen in Figure 8, no significant changes in the friction coefficient were observed on the selected distance of 2000 m, which suggests contact of the counterpart with the coating only and indirectly indicates the absence of delamination in the friction track.

Tribological studies of Ti-N coatings showed the correlation of low friction and high wear resistance with crystalline orientation. It has been shown that due to the higher packing density (111), the crystal plane of the coating is characterized by low friction.[12] Such effect was also observed for a coating formed under a pressure of 0.2 Pa, Figure 8(a).

The wear rate of the coatings is generally very low, except for the coating synthesized at 0.001 Pa of nitrogen pressure with a characteristic metallic vanadium structure, Table III. This is related with the way the coatings are deposited. Those synthesized by the cathodic arc deposition method, compared to those formed by magnetron sputtering, are characterized by better mechanical and especially tribological properties, including wear rate.[49] The differences in the wear rate may also result from different hardness and structure of tested coatings made of vanadium and nitrogen.

The hardness of the coating formed under the pressure of 0.001 Pa is small (Table III), therefore it is significantly less compared to the hardness of the applied counterpart - alumina ball. Therefore, the coating wear was abrasive. The wear width and wear depth were the greatest in comparison to the other coatings, Figure 9(a), which resulted in the big wear rate, Table III. The coatings formed at nitrogen pressure not less than 0.03 Pa have a hardness above 25 GPa, and also lower roughness, Table III. Hence, smaller wear depths and a smaller calculated wear rate. No cracks or chipping were observed in the wear tracks - they are smooth, Figures 9(b) through (d). It proves the abrasive wear of the coatings investigated.

Although the friction test was carried out in dry conditions and at room temperature, tribochemical reactions on the coating surface and a formation of oxides cannot be excluded. These oxides contribute to the improvement of the coatings abrasion resistance. The presence of vanadium oxide V_2O_5 was observed in loose wear debris in the VN coatings.[37] A similar effect, the presence of oxides in the wear debris, occurred in coatings such as CrN, MoN and TiN, *i.e.,* transition metal nitrides.[52]

The SEM and EDS image of the wear track, Figures 11(e), (f), indicate a high concentration of oxygen in the bright part of the bottom of this track. The presence of light and dark surfaces next to them suggests the possibility of a different concentration of oxygen. It was confirmed that the concentration of oxygen in dark areas is higher than in bright areas.[53] The N/V ratio is comparable in the coating and in the wear track. The oxidation of the coating during the friction test may be due to the so-called ''flash temperature'', dependent on, inter alia, normal load, sliding velocity, coating-counterpart friction coefficient, thermal conductivity of the coating and counterpart, as well as coating hardness.[54] The ''flash temperature'', taking into account the above dependencies, can reach several hundred degrees, which is sufficient for the oxidation of the coating and form a V-O tribolayer.[43,54,55]

There are two reasons for the increase in oxygen concentration in the wear track: from the Al_2O_3 counterpart material and the absorption of oxygen from the air during the friction test. The first reason is unlikely due to the absence of aluminum from the counterpart in the wear track.

The formation of areas with different oxygen concentrations may be related to their different mechanical properties. A local increase in hardness or friction coefficient observed, for example, in AlCrN coatings[56] may cause a higher flash temperature and, as a result of this catalytic phenomenon, an increase in oxygen concentration. This higher local temperature resulting from friction enables the formation of oxides in the wear track of the coating.[54] The formation of oxides characterized by different structural (crystalline system, lattice parameter), mechanical (Young's modulus, hardness), thermal (temperature coefficient of linear expansion, heat capacity) and other than coating properties can generate stresses between these layers. This allows the upper, more brittle (oxide) layer to crack.

Despite the relatively low value of H/E ratio, parameter for predicting wear resistance,[57] ranged from about 0.05 to 0.08 (excluding the coating synthesized under p_{N2} = 0.001 Pa), caused mainly by high values of Young's modulus E (365-570 GPa) does not lead to an increase in the wear rate. The wear is a complex process that can be influenced by many factors, such as grain size, crystal structure, and reactivity between the coating and the sliding material. The reduction the size of the crystallites in the coating results in an increase in hardness (Hall-Petch strengthening) and enhances the yield strength and also increases the density of the material and limits the propagation of cracks and avoids dislocations and avoids the continuity of pores in the deposited layers.[11]

The wear rate is not in line with the hardness. It should be the smallest for coatings formed under pressure in the range from 0.2 Pa to 0.8 Pa, and for other coatings characterized by lower hardness it should be higher. However, it should be noted that the adhesion of the coatings increases with nitrogen pressure and reaches the highest value for the coating formed under the pressure of 3 Pa. Thus, it confirms that adhesion, in addition to hardness, significantly affects the wear of coatings.

B. *Effect of Substrate Bias Voltage*

Many competing phenomena occur during the coating deposition. With higher substrate bias, more metal ions may be attracted to the substrate. Particles with higher kinetic energy nucleate on the substrate. The synthesized coating is denser, and this phenomenon is accompanied by the re-sputtering, as a result of which ions hitting the coating knock out atoms from it. As a result, the deposition rate is reduced and the coatings properties and their structure may change. The sputtering phenomenon is dependent on many factors, including bias, and with its increase the above results will be more visible.

Changing the phase composition of the coatings can affect the change of mechanical properties, including hardness. The modification in the structure of the coating results from the increasing energy of the ions, atoms and molecules bombarding the coating. The increase in the energy of the shot-blasted particles, resulting from the higher bias, contributes to the increase in the coatings compactness and density. This can lead to a change in the lattice parameter as shown in Figure 4(b). The coating synthesized under U_B = − 50 V shows a cubic structure, Figure 4(b), and the coatings formed at bias not lower than − 150 V have a hexagonal structure. The coating formed at U_B = − 100 V shows both of these phases. As the bias voltage increases, the lattice parameter of c-VN phase reduces, Figure 4(b). For h-VN phase, parameter a decreases, while parameter c, on the contrary, increases with increasing U_B. The change of crystallite size depends on the VN phase. For c-VN phase, the size of the crystallites decreases from approx. 30 nm to approx. 20 nm for substrate bias voltage of − 50 V and − 100 V, respectively. In case of h-VN the size of the crystallites increases from approx. 30 nm (U_B = − 100 V) to approx. 200 nm (U_B = − 300 V) is observed, Figure 4(d).

The c-VN coating has a lower hardness than h-VN coating, Table IV and Figure 3(b). In the coating formed under pressure of nitrogen of 1.5 Pa, both phases are present and its hardness is below 30 GPa. A similar relationship, higher hardness of h-VN phase coatings than c-VN phase was presented by Fallqvist and Olsson for arc-evaporated coatings.[27] It is also necessary to point out a significant increase in the crystallite size, which may be responsible for the reduction of hardness according to the Hall-Petch relationship.

Many parameters determine the use of coatings, and one of the most important is their adhesion to the substrate. One of the methods to define it is the crack test, in which the value of the normal load causing detachment of the coating from the substrate is determined, Table IV. In the coating-substrate system, there are many factors affecting the strength of its adhesion. These include: the friction coefficient in the coating - Rockwell indenter system, coating thickness, as well as the elastic properties of the substrate and wear of the indenter.[59] Therefore, identically prepared substrates from the HS6-5-2 steel were used. The coating thickness varied slightly, although, as mentioned above, the

deposition rate decrease was observed with increasing negative substrate bias voltage. All coatings were characterized by a similar nature of its damage in the scratch test. The coatings adhesion was found to be high and the critical force generally decreased with increasing negative substrate bias voltage. It is known that compressive stresses increase with increasing substrate bias voltage. Hence, as a result of bombardment with higher energy, there is a lattice mismatch and a probable reduction of the critical force. Proper substrate preparation (ionic etching) and a thin metallic vanadium adhesive transition layer are responsible for high adhesion.

The results of scratch test are confirmed by analyzing the coating damage caused by the Rockwell test. All coatings (Figure 7) show only slight radial cracks. No chipping of the coating at the indentation edge was observed. The coatings can be classified as the most resistant to damage - HF1.

High hardness and adhesion of the coatings are responsible for the high wear resistance, Table IV. Only the coating formed at $U_B = -50$ V shows a higher wear rate. It is probably connected with lower hardness, about 20 N, Table IV. The width of the wear tracks decreases with bias, which confirms the results obtained by Chen *et al.*[58]. Both the coating durability indicators, H/E[57] and H^3/E^2,[60] increase with negative bias, suggesting the wear rate decrease. The data presented in Table IV confirm this assumption. Similarly to the first series of coatings, the abrasive wear mechanism dominates.

In the initial stage (friction curve in Figure 8b), a high value of the friction coefficient is observed, which then decreases very quickly to a constant level. In the case of coatings formed with a variable substrate bias voltage, the resputtering effect should be taken into account, in which weakly bound particles are removed from the coating surface. They leave behind craters. The surface roughness can be even greater than for the coating formed under pressure of 0.2 Pa, for which the result of the friction test is shown in Figure 8(a). However, the contact surface of the coating with the counterpart, due to the small amount of macroparticles and the greater number of craters, is larger and hence the high initial value of the friction coefficient. Its decrease observed in the further stage of the friction process is probably related to the high hardness of the coating, Table IV.

V. CONCLUSION

The article shows the results of V–N coatings formation using cathodic arc evaporation method. Two sets of the coatings were synthesized: (a) In various nitrogen pressure in the working chamber and constant substrate bias voltage, (b) different substrate bias voltage and constant nitrogen pressure. The correlation between the technological parameters and the structure, mechanical and especially tribological properties of coatings deposited is presented. The analysis of the test results of both series showed a strong correlation of the above-mentioned properties with the change of both coating formation parameters, *i.e.,* nitrogen pressure and substrate bias voltage.

(a) The VN coatings deposited under nitrogen pressure from 0.001 Pa to 3 Pa are characterized by a different structure, mechanical properties. It was found that the deposition rate and nitrogen concentration in the coating increased almost linearly for p_{N2} from 0.03 Pa to 0.8 Pa. The phase transformation is also observed $V \rightarrow V + V_2N \rightarrow V + c\text{-}VN \rightarrow h\text{-}VN \rightarrow h\text{-}VN + c\text{-}VN$. The calculations also showed an increase in crystallite size and lattice parameter for the cubic phase and the opposite effect for the hexagonal phase. The Young's modulus and hardness reach maximum values of 570 GPa ($p_{N2} = 1.5$ Pa) and 37 GPa ($p_{N2} = 0.2$ Pa). An improvement in the adhesion of the coatings with pressure of nitrogen was observed. It was approx. 70 N to approx. 140 N at nitrogen pressure of 0.03 Pa to 3.0 Pa, respectively. All coatings show HF1 adhesion in the Rockwell test. Also with nitrogen pressure, the wear resistance increases by about two orders of magnitude, from about 3×10^{-5} mm^3/Nm at $p_{N2} = 0.001$ Pa to about 1.5×10^{-7} mm^3/Nm at $p_{N2} = 3$ Pa. In all cases the counterpart - Al_2O_3 ball show abrasive wear.

(b) Systematic tests of VN coatings deposited in a wide range of bias voltage from -50 V to -300 V have shown a significant influence of bias on their structural, mechanical and tribological properties. The test results indicate an almost linear decrease in the deposition rate and nitrogen concentration in the coating with the increase in the negative substrate bias voltage. This is presumably because of the resputtering phenomenon and reduces the surface roughness. There is also a c-VN $\rightarrow$ h-VN phase transition, in which a reduction in the crystallite size and the lattice parameter of the cubic phase is observe. In the case of the hexagonal phase, the opposite effect is observed. Hardness, Young's modulus also increase with U_B reaching a maximum of 37 GPa ($U_B = -200$ V) and 570 GPa ($U_B = -100$ V) respectively. This is due to the ion bombardment that grows with U_B. The high hardness is also accompanied by the high coatings adhesion, confirmed in the scratch and Rockwell tests. All coatings show HF1 adhesion. Hardness and adhesion determine the high wear resistance of the coatings. It increases, similarly to hardness, with bias, which is also confirmed by the H/E and H^3/E^2 ratios.

COMPETING INTERESTS

On behalf of all authors, the corresponding author states that there is no conflict of interest.

REFERENCES

1. K. Bobzin, T. Brögelmann, N. Stachowski, W. Hintze, C. Möller, and P. Ploog: *Materialwiss. Werkstofftech.*, 2021, vol. 52, pp. 1394–1412.
2. A. Wilczek, J. Morgiel, Ł Rogal, W. Maziarz, and J. Smolik: *Coatings*, 2020, vol. 10(3), p. 261.
3. G. Bertrand, C. Savall, and C. Meunier: *Surf. Coat. Technol.*, 1997, vol. 96, pp. 323–29.
4. H. Okamoto: *J. Phase Equilib.*, 2001, vol. 22(3), p. 362.
5. G. Farges, E. Beauprez, and D. Degout: *Surf. Coat. Technol.*, 1992, vol. 54–55, pp. 115–20.
6. T. Suszko, W. Gulbiński, A. Urbanowicz, and W. Gulbiński: *Mater. Lett.*, 2011, vol. 65, pp. 2146–48.
7. S. Kolozsvari, P. Pesch, C. Ziebert, M. Stueber, and S. Ulrich: *Plasma Process. Polym.*, 2009, vol. 6, pp. S146–51.
8. J.C. Caicedo, G. Zambrano, W. Aperador, L. Escobar-Alarcon, and E. Camps: *Appl. Surf. Sci.*, 2011, vol. 258, pp. 312–20.
9. N. Witit-Anun and A. Buranawong: *J. Met. Mater. Miner.*, 2017, vol. 27, pp. 47–52.
10. J.H. Huang, C.H. Lin, and G.P. Yu: *Thin Solid Films*, 2019, vol. 688, p. 137415.
11. L. Aissani, M. Fellah, A.H. Chadli, M.A. Samad, C. Cheriet, F. Salhi, C. Nouveau, S. Weiß, A. Obrosov, and A. Alhussein: *J. Mater. Sci.*, 2021, vol. 56, pp. 17319–36.
12. L. Aissani, A. Alhussein, C. Nouveau, L. Ghelani, and M. Zaabat: *Surf. Coat. Technol.*, 2019, vol. 378, p. 124948.
13. Y. Qiu, S. Zhang, B. Li, J.W. Lee, and D. Zhao: *Procedia Eng.*, 2012, vol. 36, pp. 217–25.
14. H. Gueddaoui, G. Schmerber, M. Abes, M. Guemmaz, and J.C. Parlebas: *Catal. Today*, 2006, vol. 13, pp. 270–74.
15. S. Bian, L. Yu, J. Xu, H. Ju, J. Wang, and H. Luo: *Appl. Phys. A*, 2022, vol. 128, p. 249.
16. Y. Feng, T.F. Chung, and J.H. Huang: *Surf. Coat. Technol.*, 2023, vol. 452, p. 129116.
17. Z. Cai, J. Pu, L. Wang, and Q. Xue: *Appl. Surf. Sci.*, 2019, vol. 481, pp. 767–76.
18. Z. Cai, J. Pu, X. Lu, X. Jiang, L. Wang, and Q. Xue: *Ceram. Int.*, 2019, vol. 45, pp. 6051–57.
19. H. Guo, B. Li, J. Wang, W. Chen, Z. Zhang, W. Wang, and J. Jia: *RSC Adv.*, 2016, vol. 6(40), pp. 33403–08.
20. H. Guo, C. Lu, Z. Zhang, B. Liang, and J. Jia: *Appl. Phys. A*, 2018, vol. 124, p. 694.
21. U. Wiklund, B. Casas, and N. Stavlid: *Wear*, 2006, vol. 261, pp. 2–8.
22. H. Hajihoseini and J.T. Gudmundsson: *J. Phys. D Appl. Phys.*, 2017, vol. 50, p. 505302.
23. L. Wang, S. Zhang, Z. Chen, J. Li, and M. Li: *Appl. Surf. Sci.*, 2012, vol. 258, pp. 3629–36.
24. R. Fix, R.G. Gordon, and D.M. Hoffman: *Chem. Mater.*, 1993, vol. 5, pp. 614–19.
25. M. Gao, X. Xu, and H. Li: *Mater. Lett.*, 2020, vol. 274, p. 128045.
26. S. Heo and W.R. Kim: *J. Korean Inst. Surf. Eng.*, 2021, vol. 54, pp. 139–43.
27. M. Fallqvist and M. Olsson: *Wear*, 2013, vol. 297, pp. 1111–19.
28. F.C. Thompson, F.M. Kustas, K.E. Coulter, and G.A. Crawford: *Surf. Coat. Technol.*, 2021, vol. 422, p. 127507.
29. Z. Cai, J. Mao, Z. Wang, W. Guo, F. Chen, Y. Dong, P. Zhang, and L. Gu: *J. Mater. Eng. Perform.*, 2023, https://doi.org/10.1007/s11665-023-07908-3.
30. J. Xu, J. Chen, and L. Yu: *Vacuum*, 2016, vol. 131, pp. 51–57.
31. J. Fan, W. Wang, H. Wang, and J. Pu: *Tribol. Lett.*, 2021, vol. 69, p. 154.
32. M.J. Rivera-Chaverra, D. Escobar, R. Ospina, M. Arroyave-Franco, J.J. Olaya, A. Pardo-Trujillo, and E. Restrepo-Parra: *Surf. Interface Anal.*, 2021, vol. 53, pp. 946–55.
33. Q. Cai, X. Bai, and J. Pu: *J. Mater. Sci.*, 2022, vol. 57, pp. 8113–26.
34. Z.X. Liu, Y. Li, X.H. Xie, J. Qin, and Y. Wang: *Ceram. Int.*, 2021, vol. 47, pp. 25655–63.
35. T. Suszko, W. Gulbiński, and J. Jagielski: *Surf. Coat. Technol.*, 2005, vol. 194, pp. 319–24.
36. J. Zhang, X. Li, X. Dong, H. Dong, A.R. Oganov, and J.M. McMahon: *Phys. Rev. B*, 2021, vol. 104, p. 134111.
37. F. Ge, P. Zhu, F. Meng, Q. Xue, and F. Huang: *Surf. Coat. Technol.*, 2014, vol. 248, pp. 81–90.
38. J.H. Huang, L.J. Wei, and I.S. Ting: *Mater. Chem. Phys.*, 2022, vol. 275, p. 125253.
39. U. Sen, M. Uzun, and S. Sen: *Adv. Mater. Res.*, 2012, vol. 445, pp. 643–48.
40. A.S. Kuprin, V.D. Ovcharenko, A. Gilewicz, G.N. Tolmachova, I.V. Kolodiy, R.L. Vasilenko, T. Kuznetsova, V. Lapitskaya, and B. Warcholinski: *Tribol. Int.*, 2022, vol. 165, p. 107246.
41. B. Warcholinski, A. Gilewicz, O. Lupicka, A.S. Kuprin, G.N. Tolmachova, V.D. Ovcharenko, I.V. Kolodiy, M. Sawczak, A.E. Kochmanska, P. Kochmanski, T.A. Kuznetsova, T.I. Zubar, A.L. Khudoley, and S.A. Chizhik: *Surf. Coat. Technol.*, 2017, vol. 309, pp. 920–30.
42. N. Vidakis, A. Antoniadis, and N. Bilalis: *J. Mater. Process. Technol.*, 2003, vol. 143–144, pp. 481–85.
43. S.J. Bull: *Tribol. Int.*, 1997, vol. 30, pp. 491–98.
44. Y. Mu, M. Liu, and Y. Zhao: *Tribol. Int.*, 2016, vol. 97, pp. 327–36.
45. B. Warcholinski, A. Gilewicz, A.S. Kuprin, and I.V. Kolodiy: *T. Nonferr. Metal. Soc.*, 2019, vol. 29, pp. 799–810.
46. G.A. Zhang, P.X. Yan, P. Wang, Y.M. Chen, and J.Y. Zhang: *Mater. Sci. Eng. A*, 2007, vol. 460–461, pp. 301–05.
47. X.S. Wan, S.S. Zhao, Y. Yang, J. Gong, and C. Sun: *Surf. Coat. Technol.*, 2010, vol. 204, pp. 1800–10.
48. P. Panjan, A. Drnovšek, P. Gselman, M. Čekada, and M. Panjan: *Coatings*, 2020, vol. 10, p. 447.
49. G.G. Fuentes, R. Rodriguez, J.C. Avelar-Batista, J. Housden, F. Montal'a, L.J. Carreras, A.B. Cristobal, J.J. Damborenea, and T.J. Tate: *J. Mater. Proc. Technol.*, 2006, vol. 167, pp. 415–21.
50. W.J. Chou, G.P. Yu, and J.H. Huang: *Surf. Coat. Technol.*, 2001, vol. 140, pp. 206–14.
51. K. Valleti, C. Rejin, and S. Joshi: *Mater. Sci. Eng. A*, 2012, vol. 545, pp. 155–61.
52. A. Öztürk, K.V. Ezirmik, K. Kazmanli, M. Ürgen, O.L. Eryilmaz, and A. Erdemir: *Tribol. Int.*, 2008, vol. 41, pp. 49–59.
53. B. Warcholinski, A. Gilewicz, P. Myslinski, E. Dobruchowska, D. Murzynski, Kochmanski, K. Rokosz, S. Raaen: *Tribol. Int.* 2021, vol. 154, p. 106744.
54. J.L. Lin, W.D. Sproul, and J.J. Moore: *Surf. Coat. Technol.*, 2012, vol. 206, pp. 2474–83.
55. M. Antonov, H. Afshari, J. Baronins, E. Adoberg, T. Raadik, and I. Hussainova: *Tribol. Int.*, 2018, vol. 118, pp. 500–14.
56. A. Gilewicz, T. Kuznetsova, S. Aizikovich, V. Lapitskaya, A. Khabarava, A. Nikolaev, and B. Warcholinski: *Materials*, 2021, vol. 14, p. 304.
57. A. Leyland and A. Matthews: *Wear*, 2000, vol. 246, pp. 1–11.
58. X. Chen, Y. Xi, J. Meng, X. Pang, and H. Yang: *J. Alloys Compd.*, 2016, vol. 665, pp. 210–17.
59. S.H. Yao and Y.L. Su: *Wear*, 1997, vol. 212, pp. 85–94.
60. J. Musil, F. Kunc, H. Zeman, and H. Polakova: *Surf. Coat. Technol.*, 2002, vol. 154, pp. 304–13.